JOURNAL OF COMPUTATIONAL PHYSICS 5, 1–12 (1970)

Low Magnetic-Field Optimisation of Focusing Device in a Helix Linear Accelerator

P. H. JUNIOR AND H. DEITINGHOFF

Institut für angewandte Physik der Universität Frankfurt/Main, Frankfurt/Main, Germany

Received May 1, 1969

ABSTRACT

A computer program is presented which is useful in designing optimal focusing devices for the synchronous particles in a nonperiodic linear accelerator. The latter is divided into sections, each containing a helix-accelerating structure and a quadrupole doublet. The helix sections of constant length differ with respect to flight times and rf conditions. Foundations are compiled, the program is discussed and an example for focusing in a low-energy accelerator is presented.

A helix linear accelerator [1–5], which is a most suitable structure for accelerating heavy ions—for instance Uranium—is the object of our studies at the "Institut für angewandte Physik" of the University of Frankfurt/Main. The high-power rf accelerating field requires water cooling of the helix, which is met in our design by a section-arrangement, where all sections have the same length of 2 m, each being followed by a magnetic quadrupole-doublet to compensate the radial defocusing forces of the rf field. Such an accelerator with constant-length focusing and defocusing elements represents a nonperiodic system with respect to the particle motion, as the flight times of the particles decrease from section to section, while the particles are gaining velocity. Therefore the fast and useful scheme of optimizing the focusing device by way of synchroton theory [6], which is valid for periodic particle motion, cannot be used in the first instance. The following analysis yields a method of computing the lowest magnetic field strengthes of the quadrupoles necessary to transport the synchronous particles from input to output of the nonperiodic accelerator. The scheme is also valid for other types of linear accelerators such as the Alvarez or Wideroe systems and in a stricter sense for the single-resonator accelerator principle, as these are neither exactly periodic, which will be shown later.

581/5/1-1

1. FOUNDATIONS

In general calculating the acceptance of an optical system—a rather intricate figure in phase space—means a necessarily tedious computational work of tracing each incoming particle to the output. An optimisation with respect to a maximum acceptance area is nearly impossible. The latter aim is made more facile by introducing elliptical acceptances [7], when the radial steering forces are linear with distance. In this approximation radial motions of synchronous particles in a helix structure are given by the equation

$$\frac{d}{dt}(\dot{r}) + \Omega_w^2 r = 0, \tag{1}$$

where

$$\Omega_w^2 = -\frac{\pi f e}{mv} E_0 \sin \varphi_s . \tag{2}$$

In the expression (2) e, m and v are the charge, mass and average velocity of the ion, respectively, while f, E_0 and φ_s are the frequency, amplitude, and synchronous phase, respectively, of the rf field. The same equation is true for motions in an Alvarez-, Wideroe-, or a single resonator-gap. In the focusing plane of a magnetic quadrupole the equation is

$$\frac{d}{dt}(\dot{r}) + \Omega_D^2 r = 0, \tag{3}$$

where

$$\Omega_D^2 = \frac{eB'}{mv}, \tag{4}$$

and B' stands for the magnetic-field gradient. When particle motions in the defocusing plane of a quadrupole are considered, Ω_D^2 is to be replaced by $-\Omega_D^2$.

The corresponding transfer matrices are

$$V = \begin{pmatrix} \cosh QW & \frac{1}{\Omega_W} \sinh QW \\ \Omega_W \sinh QW & \cosh QW \end{pmatrix}, \tag{5}$$

$$F = \begin{pmatrix} \cos QD & \frac{1}{\Omega_D} \sin QD \\ -\Omega_D \sin QD & \cos QD \end{pmatrix} \tag{6}$$

and

$$D = \begin{pmatrix} \cosh QD & \frac{1}{\Omega_D} \sinh QD \\ \Omega_D \sinh QD & \cosh QD \end{pmatrix}, \tag{7}$$

where use has been made of the rectangular hard-edged field model [8]. The flight times for passing these fields are Tw with

$$QW = T_W \cdot \Omega_W , \tag{8}$$

and T_D with

$$QD = T_D \cdot \Omega_D . \tag{9}$$

Now a linear accelerator is formed by sequences of parts represented by matrix products of the types (5), (6), (7). Examples are the $VFVD \cdots (N = 1)$ or $VFVFVDVD \cdots (N = 2)$ focusing devices, being used in most linear accelerators, presently in operation. Here all V's are nearly the same throughout the accelerator, if we neglect the $1/v$ dependence in (1) and (2), respectively. Flight times in the accelerating gaps remain constant, while the gap length increases in proportion to particle velocity. On the contrary in a helix or single resonator accelerator with constant lengths of the accelerating and focusing parts, the flight time decreases as the velocity increases, so the sequence has a form, e.g.,

$$V_1 F_1 V_2 D_2 V_3 F_3 V_4 D_4 , \qquad \text{in the } x\text{-}z\text{-plane,}$$

and

$$V_1 D_1 V_2 F_2 V_3 D_3 V_4 F_4 , \qquad \text{in the } y\text{-}z\text{-plane.}$$

Referring to (2), (4), (5), (6), (7), the V_i's, F_i's and D_i's differ from each other.

It should be emphasized that the matrices are to be put in reverse order when matrix products are to be calculated. For a periodic system synchroton theory [6] gives the elliptical acceptance in terms of the matrix elements derived from the product of one period. Here the equation of an ellipse in phase space r, dr/dt is written as

$$\beta_0 \left(\frac{dr}{dt}\right)^2 + 2\alpha_0 r \frac{dr}{dt} + \gamma_0 r^2 = \epsilon, \tag{10}$$

where ϵ is the ellipse area divided by π as long as

$$\beta_0 \gamma_0 - \alpha_0^2 = 1.$$

(10) represents the acceptance ellipse of an optical system, where one section is infinitely repeated and represented by a transfer matrix

$$A = \begin{pmatrix} a_{11} & a_{12} \\ a_{21} & a_{22} \end{pmatrix},$$

whenever we have

$$\beta_0 = \frac{a_{12}}{\sin \mu} , \qquad \gamma_0 = -\frac{a_{21}}{\sin \mu} , \qquad \alpha_0 = \frac{a_{11} - a_{22}}{2 \sin \mu} . \tag{11}$$

The characteristic exponent μ is defined by one-half the trace of A

$$\cos \mu = \frac{a_{11} + a_{22}}{2}.$$

In order to have a real acceptance ellipse, i.e., real coefficients $\alpha_0, \beta_0, \gamma_0$, the stability criterion is

$$-1 < \cos \mu < +1. \tag{12}$$

Besides a maximum area ϵ has to be chosen in such a way that the beam with an emittance (10), (11) will remain within a prescribed boundary of radius R.

Here the beam represented by (11) is investigated along the section by way of a transfer relation for elliptical beam emittances [7]

$$\begin{pmatrix} \beta(t) \\ \alpha(t) \\ \gamma(t) \end{pmatrix} = \begin{pmatrix} b_{11}^2 & -2b_{11}b_{12} & b_{12}^2 \\ -b_{11}b_{21} & b_{11}b_{22} + b_{12}b_{21} & -b_{12}b_{22} \\ b_{21}^2 & -2b_{21}b_{22} & b_{22}^2 \end{pmatrix} \begin{pmatrix} \beta_0 \\ \alpha_0 \\ \gamma_0 \end{pmatrix}, \tag{13}$$

where the elements b_{ik} occuring in (13) are to be taken from the 2×2 transfer matrix of one particle from input to this moment t. At that moment t_1, when the beam has a maximum blow up, the quantity $\beta(t_1)$ has its maximum value and the relation

$$\epsilon = \frac{R^2}{\beta(t_1)}, \tag{14}$$

is to be used.

The following table gives an insight into the variation of the characteristic parameters of 8 helix sections considered here. The section length is 200 cm, and

TABLE I

KK	$\bar{v}$ ($\cdot 10^6$ cm/sec)	E_{kin} (keV/A)	E [MV/m]	f [MHz]	T_w [$\cdot 10^{-9}$ sec]	QW
0		130.0				
1	559	200.3	0.8784	15	359.10	1.4539
2	687	285.7	1.0773	15	294.77	1.1923
3	796	374.1	1.1663	15	251.50	0.9834
4	891	456.3	1.0280	30	224.17	1.0998
5	974	537.9	1.0198	30	205.53	0.9608
6	1054	627.5	1.1193	30	189.92	0.8941
7	1135	725.2	1.2203	30	176.27	0.8350
8	1209	810.3	1.3510	30	165.39	0.7988

the example covers the low-energy part of a bigger machine for Uranium 238, designed for a final energy of 7 MeV/nucleon. The first column denotes the section number KK, E_{kin} the particle energy behind the sections, the ion charge is 11, and the synchronous phase is taken to be 30°. Evaluations indicate, that the acceptance area does not meet the requirements, when $N = 2$ or even $N = 1$ focusing is considered; therefore quadrupole doublets are taken into account and a length of 25 cm is chosen for each quadrupole. The pattern is shown in Fig. 1,

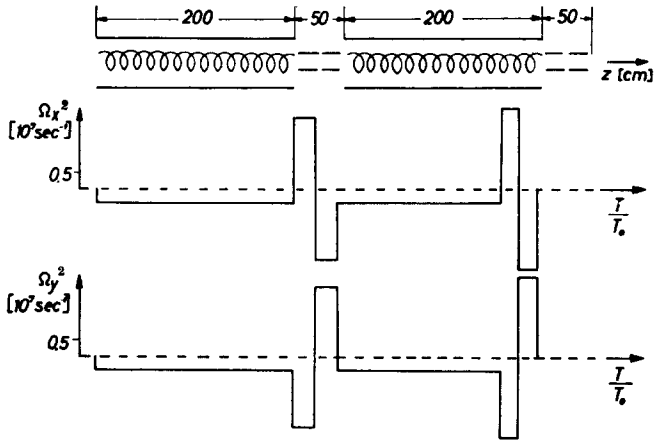

FIG. 1. Scheme of two sections of a helix linear accelerator. Each section consists of a helix part followed by a quadrupole doublet. The square of the radial frequencies Ω_x^2, Ω_y^2 corresponding to the hard-edged rectangular field approximation are drawn against the flight time.

the sequence is $V_1 F_1 D_1 V_2 F_2 D_2$,..., for the motion with respect to x, and $V_1 D_1 F_1 V_2 D_2 F_2$,..., for the motion with respect to y.

Now the objective is to evaluate a maximum acceptance of the accelerator with minimum focusing equipment. The course starts by setting the first quadrupole doublet at it's smallest strength that makes the first section stable with respect to (12). Using Eqs. (11) and (14) the corresponding acceptance ellipse is taken as the beam emittance at the input. To transmit this beam through the whole system without loss of particles the beam emittance is successively compared to the acceptances of all following sections. Tracing the beam through a new section investigations again start with the smallest quadrupol strength, that makes this section stable. If the acceptance matches the beam emittance, the beam is transmitted, in the other case another acceptance corresponding to an increased quadrupole strength is examined. The process is then repeated for a larger set of beam emittances corresponding to increased quadrupole strengthes of the first section within the stable region (12) until an optimal acceptance is found.

2. COMPUTATIONS

Each section now consists of a defocusing helix part, followed by two quadrupole parts, i.e., one focusing and one defocusing element and is characterized by a radial acceptance depending on the choice of the quadrupole lengths and their field gradients. Evaluations show that the error is small when the synchroton acceptance (11) is taken for each section instead of the general figure [9], as long as the variation of the parameters QW and Tw is small, which is the case in our example (see Table I). Therefore the acceptances for all these single sections are calculated according to the scheme (11), (14), the matrix elements being taken from the products of the matrices (5), (6), (7)

$$A = \begin{pmatrix} a_{11} & a_{12} \\ a_{21} & a_{22} \end{pmatrix} = D \cdot F \cdot V, \tag{15}$$

in x-direction and

$$B = \begin{pmatrix} a_{11} & a_{12} \\ a_{21} & a_{22} \end{pmatrix} = F \cdot D \cdot V, \tag{16}$$

in y-direction.

The process carried out is demonstrated by the flow chart Fig. 2. By aid of the given $QW = QW(KK)$ and $T_W = T(KK)$ with $KK = 1$, QD is varied from 0 upward (in steps of 0.005 in our work), until a first quantity $QD = QD1(KK)$ is found, which gives rise to fulfilment of the condition (12).

Inserting this quantity $QD1(1)$ coefficients $\alpha_1{}^A, \beta_1{}^A, \gamma_1{}^A, \epsilon_1$ are derived by aid of the Eqs. (11), (14), (15), and (16). (In our example the beam diameter should not exceed $2R = 4$ cm.) In statement number 100 the emittance of the input beam is identified with this acceptance as a consequence of the decision $KK = 1$, "YES"

$$\alpha_1{}^E = \alpha_1{}^A, \qquad \beta_1{}^E = \beta_1{}^A, \qquad \gamma_1{}^E = \gamma_1{}^A,$$

and this beam is transported through the first section denoted by the quantities $QW(1)$, $T(1)$, $QD1(1)$. The transport is carried out by means of the transfer relations (13), (15) and (16) from input to output

$$\begin{pmatrix} \beta_2{}^E \\ \alpha_2{}^E \\ \gamma_2{}^E \end{pmatrix} = \begin{pmatrix} a_{11}^2 & -2a_{11}a_{21} & a_{12}^2 \\ -a_{11}a_{21} & a_{11}a_{22} + a_{12}a_{21} & -a_{21}a_{22} \\ a_{21}^2 & -2a_{21}a_{22} & a_{22}^2 \end{pmatrix} \begin{pmatrix} \beta_1{}^E \\ \alpha_1{}^E \\ \gamma_1{}^E \end{pmatrix}, \tag{17}$$

$$\epsilon_1 = \text{const.} \tag{18}$$

Relation (18) is a consequence of Liouville's theorem.

Now the calculation of the acceptance by means of Eqs. (11) and (14) is carried out for the second section ($LL = 2$). The lowest quantity QD giving rise to a finite

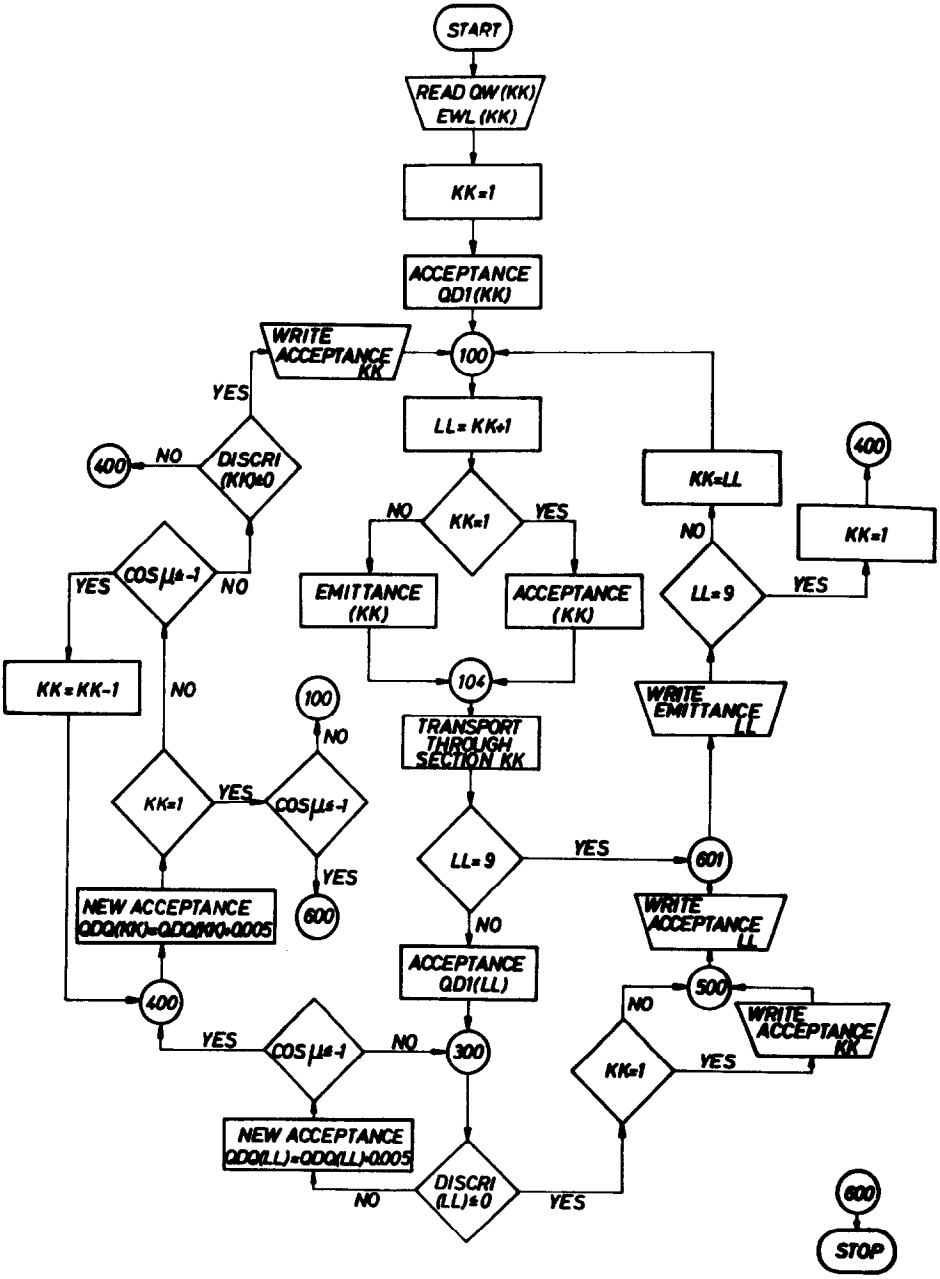

FIG. 2. Flow chart for optimal focusing of the synchronous particles in a linear accelerator.

acceptance of this section is calculated and denoted $QD1(2)$. The corresponding acceptance ellipse is characterized by the coefficients β_2^A, α_2^A, γ_2^A, ϵ_2. Entering 300 DISCRI(LL), with $LL = 2$ decides, whether the emittance ellipse β_2^E, α_2^E, γ_2^E, ϵ_1 matches the acceptance ellipse β_2^A, α_2^A, γ_2^A, ϵ_2. The criterion for this is derived by solving a forth-power equation with respect to the intersection points of those ellipses. In case of only two or no real solutions matching takes place, provided the emittance area is smaller than the acceptance area.

Naturally all this has to be done for both directions namely the x-z- and y-z-components of motion. If the ellipses fit, i.e., the decision is "YES" at 300, they are written per 500, 601 and the program continues by increasing the section number by one step. Via statement 100 the fitting emittance is again transported at 104, represented by (17); if matching did not take place at 300, the decision "NO" gives rise to a storage of the field quantity QD at this section LL by a replacement $QDQ(LL) = QD$ and another acceptance ellipse corresponding to an increased quantity $QD = QDQ(LL) + 0.005$ is calculated by way of subroutine "NEW ACCEPTANCE." The emittance is then compared to this new acceptance at 300.

In case that no acceptance ACCEPT (2) is found within (12), the flow takes its way toward 400, where a new acceptance is calculated for the preceding section $KK = 1$. For this section the field quantity has already been discussed and stored as $QDQ(1)$. By increasing $QDQ(1)$ by 0.005 transport again takes place at 100 and the acceptances $LL = KK + 1$ are successively compared to this new emittance at 300 again. The program stops at 600, if all possible acceptances of the first section have been worked through. For general section numbers KK the game is illustrated in Fig. 3.

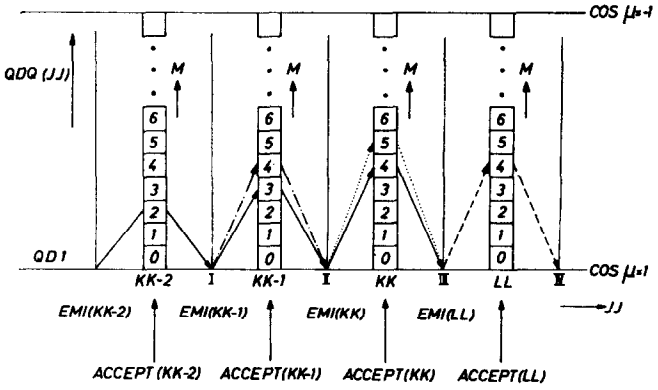

FIG. 3. Pattern to track the matching emittances and acceptances from section to section. An emittance EMI(LL) is not accepted by Section LL at III until both preceding sections $KK = LL - 1$ and $KK = LL - 2$ are operated by proper minimum-field quantities QDQ!

Assume, that the emittance EMI($KK - 2$) fits an acceptance ACCEPT($KK - 2$) with $M = 2$, where M denotes the number of steps necessary to attain $QDQ(KK - 2) = QD1(KK - 2) + 0.005\,M$, EMI($KK - 2$) is transported to I (continued line in Fig. 3) at statement 104 (Fig. 2) and denoted by EMI($KK - 1$).

Beyond that EMI($KK - 1$) should also fit ACCEPT($KK - 1$), with $M = 3$, and is denoted by EMI(KK) after transfer from I to II (continued, line Fig. 3). In the first instance EMI(KK) is assumed to match acceptance ACCEPT(KK) with $M = 4$, is then transported to III and denoted by EMI(LL), with $LL = KK + 1$ (continued line in Fig. 3).

Now assume, that no acceptance (LL) is found via 300 → DISCRI(LL) "NO" → NEW ACCEPTANCE within $-1 < \cos\mu < +1$, the preceding section (KK) will then be investigated again, while M is increased by unity ($M = 5$ now in Fig. 3) by way of Statement 400 (Fig. 2). The emittance EMI(KK) at II (Fig. 3) matched to this new acceptance ACCEPT(KK) at DISCRI(KK) < 0 "YES" is transported to III via 100 (dotted line in Fig. 3) and at last accepted by Section (LL) with $M = 4$ (dashed line in Fig. 3). In case of a decision "NO" at DISCRI(KK) new acceptances (KK) are successively worked out at 400 (Fig. 2) and matching is investigated with respect to the renowned EMI(KK). If all possibilities of Section (KK) have been checked without success, the section number, which had been KK, will again be decreased by unity per $KK = KK - 1$, and the still familiar EMI($KK - 1$) will then be compared to a new acceptance ACCEPT ($KK - 1$), which is now operated by an increased M, namely from 3 to 4 in our example (dotted and dashed line in Fig. 3) at 400 (Fig. 2). In any case emittances and acceptances will be written whenever they match, until the beam reaches the

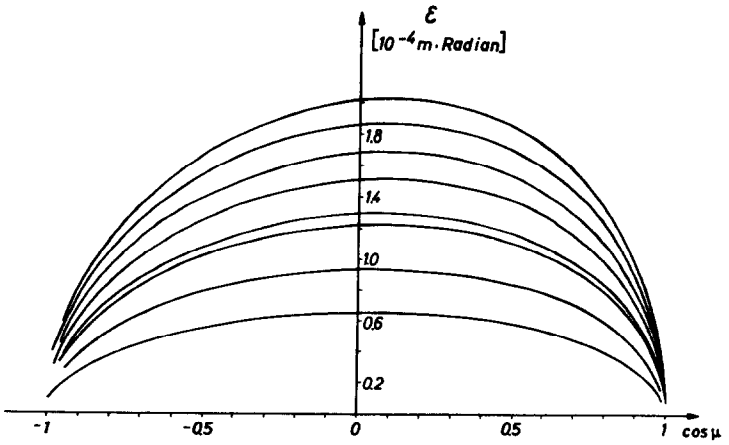

FIG. 4. Acceptance area plot as a function of $\cos\mu$ for 8 parameters QW occuring in the example presented here.

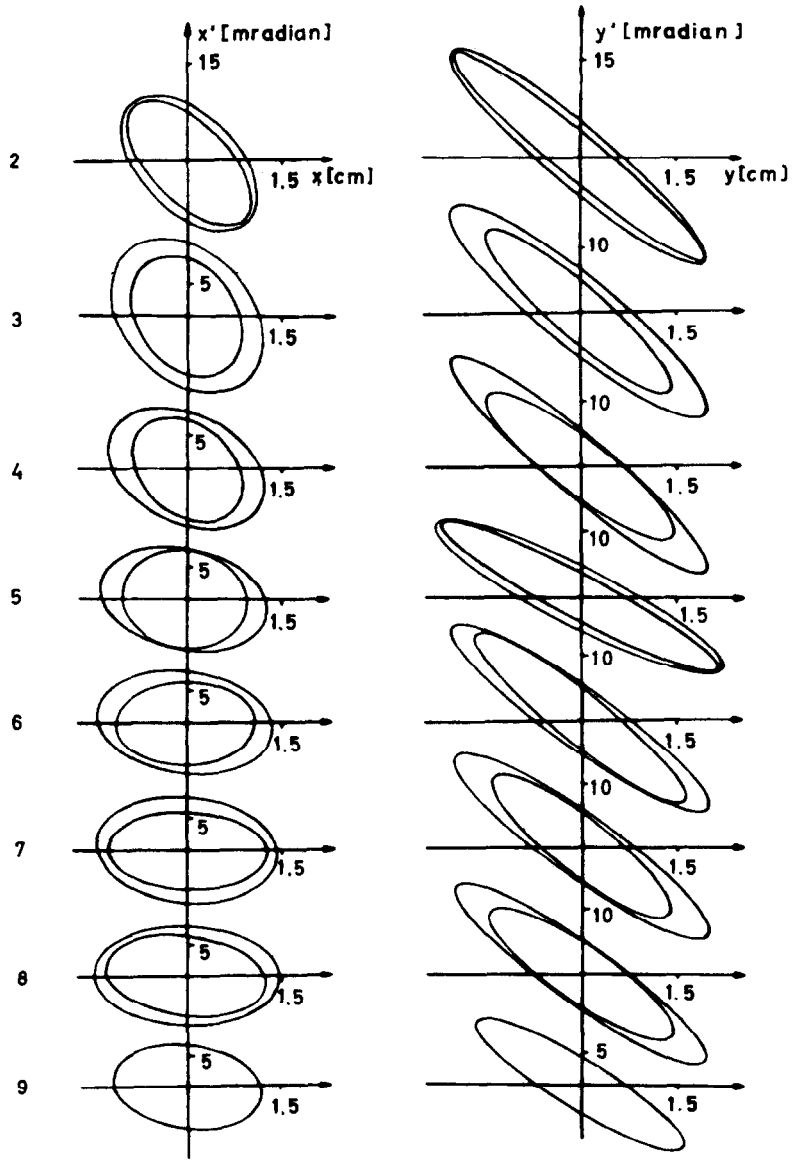

FIG. 5. Matched emittance and acceptance ellipses between the sections. On the left-hand side the ellipses correspond to the x- and the right-hand side to the y-direction. For both directions the areas are identical.

designed final energy. By way of the decision $LL = 9$, "YES" the emittance of the output beam is written at 601 and by way of statement $KK = 1$ a new acceptance and the corresponding emittance obtained by an increased $M = M + 1$ at the input is tracked through the accelerator until all focusing field gradients of interest—for instance within $-\frac{1}{2} < \cos\mu < +\frac{1}{2}$—have been taken care of.

RESULTS

Calculations have been carried out for a set of quantities QD in steps of 0.005, delivering reasonable acceptance areas ϵ depending on the characteristic exponent for given parameters QW. These areas are displayed in Fig. 4. It turns out, that maximum acceptance areas are not achieved exactly at $\cos\mu = 0$ but at small positive values. In our example $\cos\mu = 0.06$ determines a maximum acceptance area of 6.6 cm · mrad with a maximum beam diameter of $2R = 4$ cm for the first section, being simultaneously the optimal acceptance of the low-energy design in Fig. 1. The matching acceptance ellipses and the resulting beam emittances for each section are displayed in Fig. 5. In Fig. 6 the functions QW, $QD1$, QD, $\cos\mu$ and B' are plotted against the section number. Some interesting behavior occures at section number 4, where the duplicated *rf* frequency (Table I) interrupts the monotony of the argument QW, causing a disturbance in the steady rise of $\cos\mu$ already at section number 3. As a consequence the field gradient B' has to be

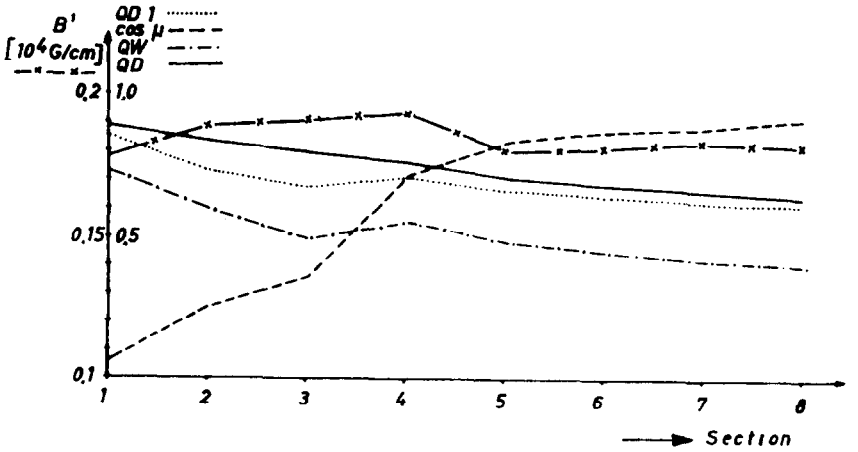

FIG. 6. Plot of significant quantities as functions of the section number, namely the given arguments QW, the smallest field quantities $QD1$ to attain $\cos\mu$ within (12), the smallest field quantities QDQ to match acceptances and emittances throughout the accelerator and the corresponding field gradients B' of the magnetic quadrupoles.

slightly increased here and the y-ellipses in Fig. 5 do not touch each other contrary to their behaviour at all other sections.

The inner ellipses at $LL = 2$ correspond to the input acceptance, the output beam is described by the single ellipses at $LL = 9$. All areas and ellipses displayed in Fig. 4 and 5, respectively, are calculated in units of cm · mrad with reference to an input particle energy of 130 keV/A. The programs have been written in Fortran IV language, the computations have been carried out by an IBM 7094 computer at the DRZ Darmstadt, Germany. The machine time used in our example was 6.25 min., calculating focusing designs for a bigger accelerator up to a final energy of 7 MeV/A time did not exceed 30 min. in any case.

ACKNOWLEDGMENT

We are much obliged to Mrs. Marion Herzfeldt for her careful drawings.

REFERENCES

1. W. WALKINSHAW AND K. WYLLIE, *Maths. Memo.*/57/WW (TRE) (1948).
2. K. JOHNSEN AND H. DAHL, *Chr. Michelsens Inst. Beretn.* **XIV**, 4 (1951).
3. H. KLEIN, *Z. angew. Physik* **18**, 143 (1964). Translation: Atomic Energy of Canada Ltd., AECL-2287 (1965).
4. H. DÄNZER AND H. KLEIN, Der Wendelbeschleuniger für schwere Ionen, Interner Bericht (1968). Institut für angewandte Physik, Frankfurt/Main.
5. H. KLEIN, Die Beschleunigung schwerer Ionen mit der Wendelstruktur, Interner Bericht (1968). Institut für angewandte Physik, Frankfurt/Main.
6. E. D. COURANT AND H. S. SNYDER, *Ann. Phys.* **3**, 1 (1958).
7. K. G. STEFFEN, "High Energy Beam Optics." Wiley (Interscience) (1965).
8. A. SEPTIER, "Advances in Electronics and Electron Physics XIV." Academic Press, New York (1961).
9. P. JUNIOR, *Z. angew. Physik* **25**, 117 (1968).